Sexual dimorphism of synaptonemal complex length in threespine stickleback fish

Barquiesha S. Madison[*], Mary K. Flanagan[*], Shivangi Nath[*], and Michael A. White[*]

[*]Department of Genetics, University of Georgia, Athens, GA, 30602

Corresponding author:

Michael A. White

Department of Genetics, University of Georgia

120 Green St.

Athens, GA 30602

whitem@uga.edu

Abstract

Crossover frequency often differs substantially between sexes (i.e. heterochiasmy). Although this phenomenon is widespread throughout taxa, the mechanisms that lead to heterochiasmy remain unclear. One pattern that has emerged is that the overall length of the synaptonemal complex likely has a direct influence on the total number of crossovers in each sex. However, this has only been investigated in a handful of species. The threespine stickleback fish *(Gasterosteus aculeatus)* is an excellent species to explore whether synaptonemal complex length is associated with a difference in the total number of crossovers, as females have longer linkage maps than males. We used immunocytogenetics to quantify synaptonemal complex length in late pachytene female and male meiocytes. We found that females had synaptonemal complexes that were 1.65 times longer than males, which is remarkably similar to the length difference observed in a sex-specific linkage map constructed from a cross between two other populations. Our results support a model where chromosome axis length determines overall crossover frequency and establish the threespine stickleback as a useful species to explore the mechanistic basis of heterochiasmy.

Key words: Threespine stickleback fish, sexual dimorphism, meiosis, synaptonemal complex

Introduction

Crossing over is an essential step of meiosis that is required for the proper pairing and segregation of homologous chromosomes. At minimum, a single crossover is typically required per chromosome or chromosome arm for meiosis to complete correctly [1–4]. Errors during crossover formation may lead to severe segregation errors resulting in aneuploidies [5]. Beyond this minimum requirement, the overall frequency at which this essential process occurs throughout the genome can vary tremendously. Genome-wide rates of crossing over are highly variable between species and even within species (reviewed in [6–8]), with some of the greatest differences occurring between sexes (i.e. heterochiasmy; reviewed in [9]).

The mechanism that leads to rate differences between sexes is unclear. However, the chromatin environment imposed by the synaptonemal complex (SC) likely plays a role. The SC is a proteinaceous axis that links homologous chromosomes together at mid-prophase (reviewed in [10]). This structure serves as a scaffold in which DNA double strand breaks are repaired between homologous chromosomes in a crossover or non-crossover fashion. There is a strong positive correlation between crossover number and the total length of the SC [11–18], suggesting that this structure may directly determine the overall frequency of crossover events. Even among individuals within a species, SC length can vary widely [19,20], altering the organization of DNA along the chromosome axis [21–23]**.** The same length of DNA organized along a longer chromosome axis, results in smaller chromatin loops and a higher frequency of crossover formation.

Heterochiasmy in some species is correlated with sex-specific differences in SC length. In mammals, females exhibit longer SC complexes, coincident with higher crossover frequencies, relative to males [11–13]. Heterochiasmy is widespread in plants and animals

(reviewed in [9]), yet it remains unknown whether altered SC length is a universal mechanism responsible for this phenomenon. Outside of mammals, dimorphic SC lengths have only been noted in teleost fish, and these analyses have revealed conflicting patterns. Zebrafish have been shown to have longer SC lengths in female fish, congruent with a higher frequency of crossing over [14]. However, in cichlid fish there has been no consistent pattern identified between SC length and the sex-specific frequency of crossing over [24]. Additional teleost species are needed to assess the generality of these mechanisms.

Similar to other organisms, threespine stickleback fish *(Gasterosteus aculeatus)* exhibit striking dimorphism in crossover frequency between males and females. Sex-specific linkage maps in this species have shown females have crossover frequencies that are 1.64 times higher relative to males [25]. Despite these differences in crossover frequency, there is no evidence of dimorphic SC lengths. Chromosome axis lengths have been measured in a single freshwater river population of fish using electron microscopy [26]. In this population, males and females had axes of similar length at pachytene. Because these two studies used different source populations, it raises the possibility that sexual dimorphism of SC lengths may be polymorphic, increasing female crossover frequency in select populations. Alternatively, SC lengths may not be dimorphic in threespine stickleback fish, and heterochiasmy may be driven by an independent mechanism. Here, we use immunocytogenetics to characterize male and female SC length in a marine population of threespine stickleback fish. Unlike the previous study, we document a significantly longer SC in females, relative to males. Our results align with sex-specific linkage maps in threespine stickleback [25] and suggest changes in SC length may be responsible for the altered crossover landscape between sexes in some populations.

Materials and Methods

Ethics statement

All procedures using threespine stickleback fish were approved by the University of Georgia Animal Care and Use Committee (protocol A2018 10-003-Y2-A5).

Preparation of meiotic chromosome spreads from threespine stickleback fish

Meiotic chromosome spreads were isolated from male and female threespine stickleback fish following previously established protocols from mice [27] and teleost fish [28]. Threespine stickleback fish exhibit seasonal gametogenesis [29–31]. Therefore, we targeted stages of juvenile development when meiosis was actively occurring in male and female fish. This was determined to occur between five and six months after hatch. The gonads were dissected from five male fish and five female fish, isolated from a lab population of wild-caught fish from Port Gardner Bay (Everett, Washington, USA). The gonads were immersed in 500 µl of phosphate-buffered saline (PBS), and minced into a fine cell solution using a dounce homogenizer with a small clearance pestle. To account for fewer meiocytes, all ovaries were pooled into a single sample for homogenization. Testes were homogenized as one sample per male. The cell solution was centrifuged at 500 xg for five minutes to pellet the cells. After centrifugation, the supernatant was discarded, and the pellet was resuspended in one of two hypotonic solutions. For females, we used 100 µl of 0.8% sodium citrate and the suspension was incubated at room temperature for twenty minutes. For males, we used 100 µl of 100 mM sucrose and the suspension was incubated at room temperature for twenty minutes. The different hypotonic solutions were used because 0.8% sodium citrate did not result in clear chromosome spreads in males. Importantly, synaptonemal complex length is not significantly affected by the type of

hypotonic solution (Figure S1). After incubating, 20 µl of the female cell solution and 20 µl of sucrose was placed and mixed on a microscope slide. For the male solution, 20 µl of the cell solution was placed on a microscope slide without sucrose. Slides from both sexes were fixed by adding 100 µl of 1% paraformaldehyde with 0.15% TritonX-100 and were incubated at room temperature for 2.5 hours in a covered, humidified chamber. After incubating, we removed the slides from the humidified chamber and allowed them to dry overnight. After drying, the slides were washed three times with a fresh solution of 1X PBS (15 minutes, 10 minutes, then 5 minutes). The slides were air-dried and immediately processed for immunofluorescence or stored at -20°C. Stored slides were all used within two weeks, the time period where they produce optimal results [27].

Immunofluorescence of axial elements of the synaptonemal complex

We visualized the localization of a cohesin protein (structural maintenance of chromosomes 3; SMC3) within the axial elements that associate sister chromatids (reviewed in [32]). Samples were first permeabilized for 20 minutes using permeabilization solution (1X PBS, 1mM EDTA, and 1% TritonX-100) [33]. The solution was drained from the slide and 1.5 ml of 1X antibody dilution buffer (1X PBS, 0.25% normal goat serum, 0.003 g/ml BSA, and 0.005% TritonX-100) was added and incubated for 20 minutes [34]. A 1:100 dilution of ice-cold primary anti-SMC3 (Abcam; ab9263) was added onto the slide and sealed with a coverslip and rubber cement. The primary antibody was incubated at 4°C overnight. The coverslip was removed by immersion in 1X PBS. 1.5ml of 1X antibody dilution buffer was added to the slide and incubated for 20 minutes. After incubation, a 1:100 dilution of goat anti-rabbit (Abcam; ab150077) was added, the slide was sealed with a coverslip and rubber cement, and the sealed slide was

incubated at 37°C for two to three hours. Slides were washed three times in 1X PBS. After the slides were washed, 40 µl of 1X 4',6-diamidino-2-phenylindole (DAPI; Biotium) was added and the slides were sealed with a coverslip and clear nail polish.

Imaging and measuring synaptonemal complex length

Cells were visualized using a Leica DM6000 B upright microscope at 63x magnification with DAPI and FITC filter sets. Images were captured using a Hamamatsu ORCA-ER digital camera. A total of 41 oocytes and 134 spermatocytes were determined to be within prophase I of meiosis. We staged each meiocyte to their corresponding substage of prophase I according to the overall organization of the synaptonemal complex, revealed by SMC3 localization. Spreads showing sparse SMC3 localization were characterized as leptotene, spreads with fully formed SMC3 axes, but did not show fully synapsed homologs (having a chromosome count greater than n=21) were characterized as zygotene, and spreads with fully formed SMC3 axes and a chromosome count of 21 were characterized as late pachytene. Only male and female cells that were in late pachytene were used to quantify the synaptonemal complex lengths. At this stage, the synaptonemal complex is fully formed and chromosomes are completely paired. The length of each synaptonemal complex was measured in pixels using the freehand line tool and measure function of ImageJ software [35,36]. We were blinded to the sex of each sample before measuring. Pixel-based lengths of each chromosome were converted to microns based on a conversion factor specific to the digital camera and camera adapter.

Results and Discussion

Males and females exhibit fully synapsed homologs at pachytene

Threespine stickleback fish have heteromorphic X and Y chromosomes that have diverged from one another [37–40]. In some species with heteromorphic sex chromosomes, synapsis is limited to the short pseudoautosomal region, leaving the remainder unpaired between homologs [41–43]. We therefore first wanted to explore whether males exhibit any differences in synapsis among chromosomes. We targeted structural maintenance of chromosomes 3 (SMC3), a protein important for the cohesion of sister chromatids during meiosis (reviewed in [32]) and characterized the different substages of prophase I. In total, we staged 134 spermatocytes and 41 oocytes to leptotene, zygotene, or late pachytene (Figure 1). From the total pool, 16 spermatocytes and 11 oocytes were in late pachytene of meiosis I. We found meiocytes where males and females had a total of 21 fully synapsed chromosomes, consistent with the haploid chromosome count in threespine stickleback fish [44]. Our results indicate the X and Y chromosomes must be fully synapsing in a non-homologous fashion within a large proportion of meiocytes, similar to what was previously observed using electron microscopy [26].

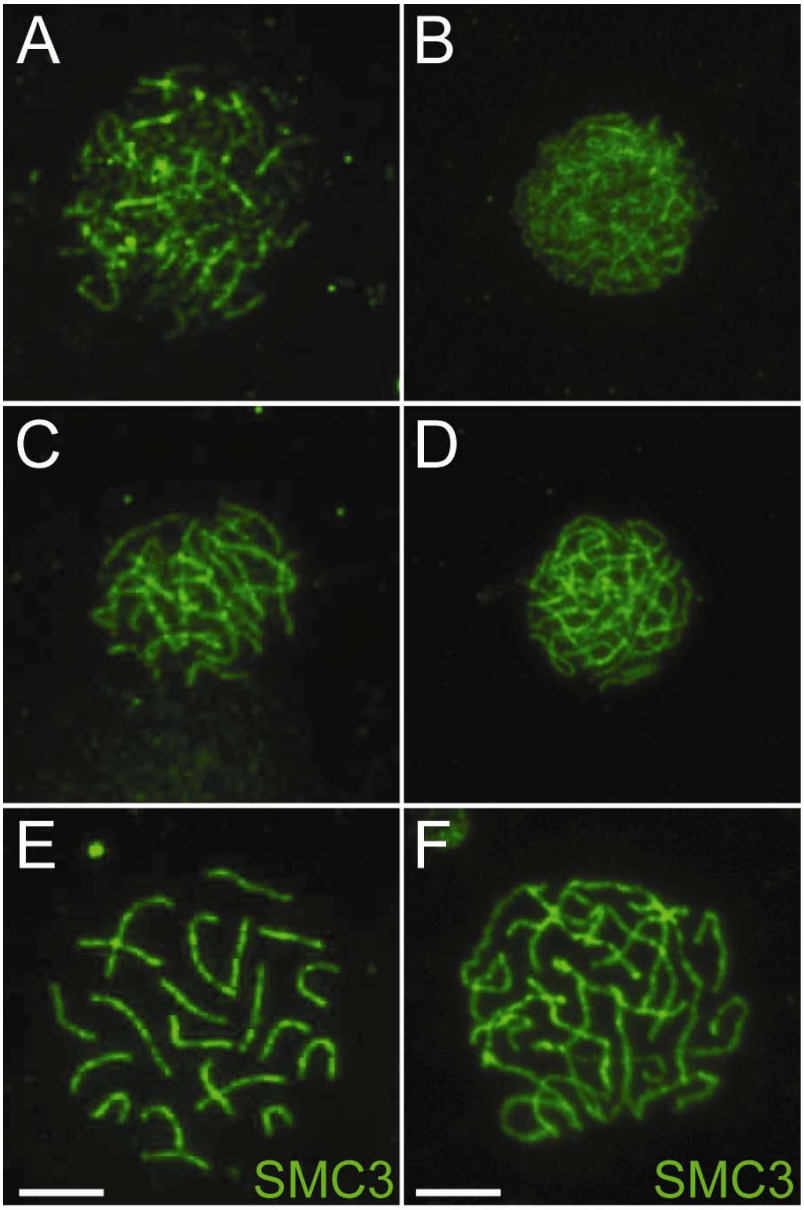

Figure 1. Progression of synapsis throughout prophase in female and male meiocytes. Axial elements of the synaptonemal complex are labeled for localization of the cohesion protein, SMC3 during (A) male leptotene, (B) female leptotene, (C) male zygotene, (D) female zygotene, (E) male pachytene, and (F) female pachytene. Scale bars represent 5 µm.

Highly degenerate, ancient sex chromosomes exhibit delayed pairing and repair of double strand breaks during meiosis due to an overall lack of sequence homology between the X and Y chromosomes [45–47]. Recently derived sex chromosomes have higher sequence homology, which could facilitate full synapsis. For example, the young X and Y chromosomes of guppy fish

fully synapse, albeit in a delayed fashion relative to autosomes [48]. The threespine stickleback Y chromosome also has higher sequence homology between the X and Y chromosomes compared to the ancient sex chromosomes of mammals [39,40]. However, there is also substantial structural divergence between the threespine stickleback X and Y, with at least three major inversions that disrupt sequence collinearity between the two chromosomes [38,39]. It is unclear how the X and Y still synapse fully despite the inversions. It is possible the inversions and sequence divergence may delay pairing and lead to a failure of synapsis in a subset of meiocytes. Our current approach cannot determine how divergence at the nucleotide and structural level affects overall timing and extent of pairing between the heteromorphic X and Y chromosomes. DNA fluorescent in situ hybridization (FISH) probes for the sex chromosomes will be needed to test whether unpaired or partially paired sex chromosomes are enriched in the pool of spermatocytes that did not exhibit full synapsis of all 21 chromosomes.

Females have longer synaptonemal complexes at pachytene

Female threespine stickleback fish have longer genetic map lengths, relative to males [25]. In many species, sex-specific crossover frequencies are highly correlated with overall synaptonemal complex length at pachytene [11–14,49]. We investigated whether threespine stickleback fish also exhibit sexual dimorphism of SC length by measuring SMC3 labeled chromosome axes. Female fish had a significantly longer total axis length at pachytene compared to males (1.65x longer in females; Figure 2; Table S1; t-test, $P < 0.001$), with greater variability among meiocytes in females (female SD: 25.562; male SD: 15.718). The total length difference does not appear to be driven by a small subset of chromosomes, as the increase in synaptonemal

complex length was still highly apparent when assayed per chromosome (Figure 2; Table S2; t-test, $P < 0.001$).

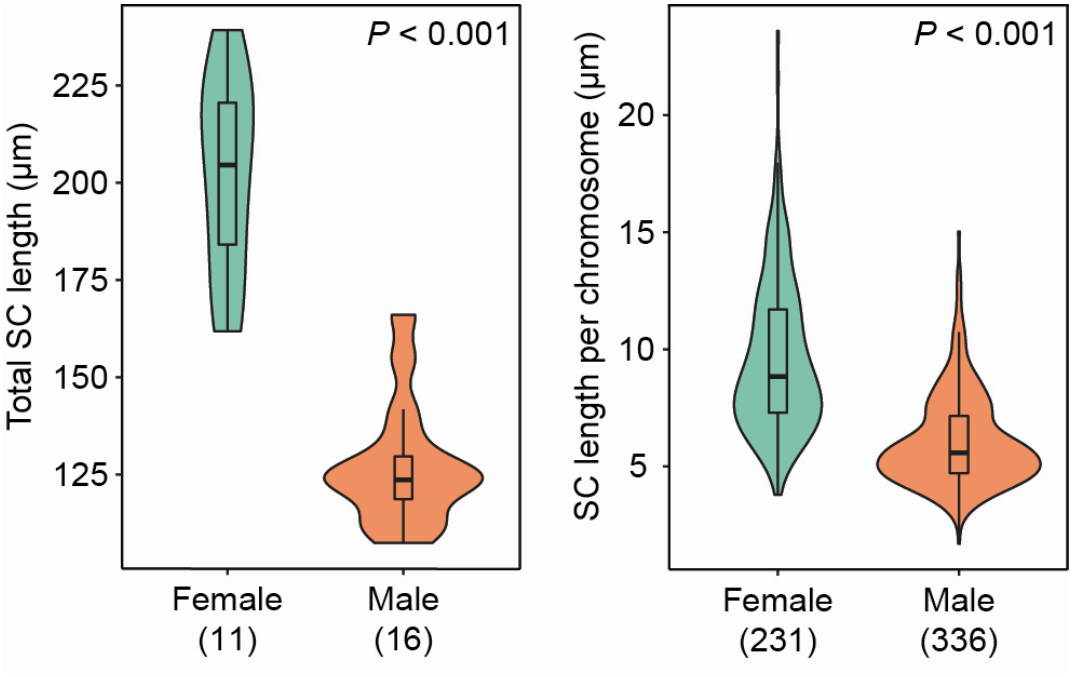

Figure 2. Females have longer synaptonemal complexes than males at late pachytene. Total length of SMC3 label along the synaptonemal complex was measured at late pachytene. The total number of measured fish or the total number of measured chromosomes is indicated below the plots. Whiskers denote 1.5x the interquartile range.

The length difference we observed was remarkably similar to the difference in sex-specific genetic maps in crosses between two different marine populations of threespine stickleback fish (1.65x longer SC in females; 1.64x longer genetic map in females; [25]). Our results indicate sex-specific crossover frequency may be highly correlated with overall SC length in threespine stickleback, as observed in mammals and zebrafish [11–14,49]. Our results stand in contrast with previous measurements of SC length in a freshwater river population of threespine stickleback fish [26]. Males in the river population had a mean SC length (150 ± 18 µm) that fell in range of our measurements. However, mean SC length in females (143 ± 12 µm) was considerably lower than our estimates. One possibility is there is polymorphism among

populations of threespine stickleback in overall SC length. Variation in SC length has been documented between closely related species [12,12,17,18,24] and within species [20]. In house mice, within species variation in male SC length has been associated with multiple quantitative trait loci [19,20]. If threespine stickleback fish have a similar genetic architecture shaping SC length, alternate alleles at these loci may have diverged between populations, leading to the observed polymorphism. Additional population sampling will be necessary to test this hypothesis.

Sex-specific crossover frequency can also vary at a fine scale throughout the genome. Males often exhibit a higher frequency of crossovers towards the ends of chromosomes, whereas females have a more uniform distribution [16,49–57]. An outstanding question is whether these regional shifts in crossover frequency between sexes are also associated with sexual dimorphism of SC length. The only regional difference in SC length between sexes has been examined in the house mouse pseudoautosomal region [58], the small region of sequence homology between the X and Y that experiences exceptionally high rates of crossing over in males [59]. The pseudoautosomal region has an extended chromosome axis compared to the ends of some autosomes [46]. However, this extended axis does not appear to be sex-specific, as it is also found in female meiocytes, where recombination on the X chromosome is not restricted to the pseudoautosomal region [58]. This makes it unclear whether dimorphic SC lengths are responsible for heterochiasmy across specific regions of chromosomes. Threespine stickleback also exhibit heterochiasmy at a fine scale, with elevated crossover frequencies at the ends of chromosomes in males relative to females [25]. They will therefore be a useful species to further explore the mechanisms leading to regional differences in heterochiasmy along chromosomes.

Conclusions

Our results reveal threespine stickleback fish have substantial differences in SC length between males and females in a marine population, supporting a model that the chromatin environment imposed by the SC may be responsible for sexually dimorphic crossover frequencies. The differences observed between this study and previous work in a river ecotype highlight that SC lengths may vary considerably among populations. Future work focusing on variation among populations will shed light on the genetic basis of SC length variation and its relationship with crossover frequency.

Supplementary Materials

Figure S1: The effect of hypotonic solution on synaptonemal complex length in males.

Table S1: Total length of the synaptonemal complex for each male and female fish.

Table S2: Length of the synaptonemal complex for each of the 21 paired homologs in male and female fish.

Acknowledgements

The authors thank Lucille Welch for help imaging the female meiocytes. The authors acknowledge the following funding sources: National Science Foundation MCB 1943283 (MAW), Office of the Vice President of Research at the University of Georgia (MAW), and the Rosemary Grant Advanced award from the Society for the Study of Evolution (SN).

Author contributions

Conceptualization, S.N. and M.A.W.; Methodology, S.N., B.M., and M.A.W.; Formal Analysis, S.N., B.M., M.F., and M.A.W.; Investigation, S.N. and B.M.; Resources, M.A.W.; Writing – Original Draft Preparation, B.M. and M.A.W.; Writing – Review & Editing, S.N., B.M., M.F., and M.A.W.; Visualization, B.M. and M.A.W.; Supervision, S.N. and M.A.W.; Project Administration, M.A.W.; Funding Acquisition, S.N. and M.A.W.

Conflicts of Interest

The authors declare no conflicts of interest.

References

1. Dumont, B.L. Variation and Evolution of the Meiotic Requirement for Crossing Over in Mammals. *Genetics* **2017**, *205*, 155–168, doi:10.1534/genetics.116.192690.

2. Sun, F.; Oliver-Bonet, M.; Liehr, T.; Starke, H.; Ko, E.; Rademaker, A.; Navarro, J.; Benet, J.; Martin, R.H. Human male recombination maps for individual chromosomes. *Am J Hum Genet* **2004**, *74*, 521–531, doi:10.1086/382138.

3. Villena, F.P.-M. de; Sapienza, C. Recombination is proportional to the number of chromosome arms in mammals. *Mamm Genome* **2001**, *12*, 318–322, doi:10.1007/s003350020005.

4. Segura, J.; Ferretti, L.; Ramos-Onsins, S.; Capilla, L.; Farré, M.; Reis, F.; Oliver-Bonet, M.; Fernández-Bellón, H.; Garcia, F.; Garcia-Caldés, M.; et al. Evolution of recombination in eutherian mammals: insights into mechanisms that affect recombination rates and crossover interference. *Proc Royal Soc B Biological Sci* **2013**, *280*, 20131945, doi:10.1098/rspb.2013.1945.

5. Hassold, T.; Hunt, P. To err (meiotically) is human: the genesis of human aneuploidy. *Nature Reviews Genetics* **2001**, *2*, 280-291, doi:10.1038/35066065.

6. Coop, G.; Przeworski, M. An evolutionary view of human recombination. *Nat Rev Genet* **2007**, *8*, 23-34, doi:10.1038/nrg1947.

7. Smukowski, C.S.; Noor, M.A.F. Recombination rate variation in closely related species. *Heredity* **2011**, *107*, 496–508, doi:10.1038/hdy.2011.44.

8. Ritz, K.R.; Noor, M.A.F.; Singh, N.D. Variation in Recombination Rate: Adaptive or Not? *Trends Genet* **2017**, *33*, 364–374, doi:10.1016/j.tig.2017.03.003.

9. Sardell, J.M.; Kirkpatrick, M. Sex differences in the recombination landscape. *Am Nat* **2020**, 95, 361-379, doi:10.1086/704943.

10. Page, S.L.; Hawley, R.S. The genetics and molecular biology of the synaptonemal complex. *Annu Rev Cell Dev Bi* **2004**, *20*, 525–558, doi:10.1146/annurev.cellbio.19.111301.155141.

11. Tease, C.; Hultén, M.A. Inter-sex variation in synaptonemal complex lengths largely determine the different recombination rates in male and female germ cells. *Cytogenet Genome Res* **2004**, *107*, 208-215, doi:10.1159/000080599.

12. Lynn, A.; Koehler, K.E.; Judis, L.; Chan, E.R.; Cherry, J.P.; Schwartz, S.; Seftel, A.; Hunt, P.A.; Hassold, T.J. Covariation of Synaptonemal Complex Length and Mammalian Meiotic Exchange Rates. *Science* **2002**, *296*, 2222-2225, doi:10.1126/science.1071220.

13. Gruhn, J.R.; Rubio, C.; Broman, K.W.; Hunt, P.A.; Hassold, T. Cytological Studies of Human Meiosis: Sex-Specific Differences in Recombination Originate at, or Prior to, Establishment of Double-Strand Breaks. *PLoS ONE* **2013**, *8*, e85075, doi:10.1371/journal.pone.0085075.

14. Kochakpour, N.; Moens, P.B. Sex-specific crossover patterns in Zebrafish (*Danio rerio*). *Heredity* **2008**, *100*, 489-495, doi:10.1038/sj.hdy.6801091.

15. Drouaud, J.; Mercier, R.; Chelysheva, L.; Bérard, A.; Falque, M.; Martin, O.; Zanni, V.; Brunel, D.; Mézard, C. Sex-Specific Crossover Distributions and Variations in Interference Level along *Arabidopsis thaliana* Chromosome 4. *Plos Genet* **2007**, *3*, e106, doi:10.1371/journal.pgen.0030106.

16. Giraut, L.; Falque, M.; Drouaud, J.; Pereira, L.; Martin, O.C.; Mézard, C. Genome-Wide Crossover Distribution in Arabidopsis thaliana Meiosis Reveals Sex-Specific Patterns along Chromosomes. *Plos Genet* **2011**, *7*, e1002354, doi:10.1371/journal.pgen.1002354.

17. Ruiz-Herrera, A.; Vozdova, M.; Fernández, J.; Sebestova, H.; Capilla, L.; Frohlich, J.; Vara, C.; Hernández-Marsal, A.; Sipek, J.; Robinson, T.J.; et al. Recombination correlates with synaptonemal complex length and chromatin loop size in bovids—insights into mammalian meiotic chromosomal organization. *Chromosoma* **2017**, *126*, 615–631, doi:10.1007/s00412-016-0624-3.

18. Fröhlich, J.; Vozdova, M.; Kubickova, S.; Cernohorska, H.; Sebestova, H.; Rubes, J. Variation of Meiotic Recombination Rates and MLH1 Foci Distribution in Spermatocytes of Cattle, Sheep and Goats. *Cytogenet Genome Res* **2015**, *146*, 211–221, doi:10.1159/000439452.

19. Pan, Z.; Yang, Q.; Ye, N.; Wang, L.; Li, J.; Yu, D.; Cooke, H.J.; Shi, Q. Complex relationship between meiotic recombination frequency and autosomal synaptonemal complex length per cell in normal human males. *Am J Med Genet A* **2012**, *158A*, 581–587, doi:10.1002/ajmg.a.35222.

20. Wang, R.J.; Dumont, B.L.; Jing, P.; Payseur, B.A. A first genetic portrait of synaptonemal complex variation. *PLOS Genetics* **2019**, *15*, e1008337, doi:10.1371/journal.pgen.1008337.

21. Kauppi, L.; Jasin, M.; Keeney, S. The tricky path to recombining X and Y chromosomes in meiosis. *Annals of the New York Academy of Sciences* **2012**, *1267*, 18-23, doi:10.1111/j.1749-6632.2012.06593.x.

22. Kleckner, N.; Storlazzi, A.; Zickler, D. Coordinate variation in meiotic pachytene SC length and total crossover/chiasma frequency under conditions of constant DNA length. *Trends Genet* **2003**, *19*, 623–628, doi:10.1016/j.tig.2003.09.004.

23. Blat, Y.; Protacio, R.U.; Hunter, N.; Kleckner, N. Physical and functional interactions among basic chromosome organizational features govern early steps of meiotic chiasma formation. *Cell* **2002**, *111*, 791-802, doi:10.1016/s0092-8674(02)01167-4.

24. Campos-Ramos, R.; Harvey, S.C.; Penman, D.J. Sex-specific differences in the synaptonemal complex in the genus Oreochromis (Cichlidae). *Genetica* **2009**, *135*, 325–332, doi:10.1007/s10709-008-9280-8.

25. Sardell, J.M.; Cheng, C.; Dagilis, A.J.; Ishikawa, A.; Kitano, J.; Peichel, C.L.; Kirkpatrick, M. Sex Differences in Recombination in Sticklebacks. *G3* **2018**, *8*, 1971–1983, doi:10.1534/g3.118.200166.

26. Cuñado, N.; Barrios, J.; Miguel, E.S.; Amaro, R.; Fernández, C.; Hermida, M.; Santos, J.L. Synaptonemal Complex Analysis in Oocytes and Spermatocytes of Threespine Stickleback *Gasterosteus Aculeatus* (Teleostei, Gasterosteidae). *Genetica* **2002**, *114*, 53-56, doi:10.1023/a:1014685114092.

27. Dia, F.; Strange, T.; Liang, J.; Hamilton, J.; Berkowitz, K.M. Preparation of Meiotic Chromosome Spreads from Mouse Spermatocytes. *Journal of Visualized Experiments* **2017**, 129, e55378, doi:10.3791/55378.

28. Araya-Jaime, C.; Serrano, É.A.; Silva, D.M.Z. de A.; Yamashita, M.; Iwai, T.; Oliveira, C.; Foresti, F. Surface-spreading technique of meiotic cells and immunodetection of synaptonemal complex proteins in teleostean fishes. *Molecular Cytogenetics* **2015**, *8*, 4, doi:10.1186/s13039-015-0108-9.

29. Craig-Bennett, A. The reproductive cycle of the threespined stickleback, *Gasterosteus aculeatus*, Linn. *Phil. Trans. Roy. Soc. B.* **1931**, *219*, 197-279, doi:10.2307/92176.

30. Borg, B. Seasonal effects of photoperiod and temperature on spermatogenesis and male secondary sexual characters in the three-spined stickleback, *Gasterosteus aculeatus* L. *Canadian Journal of Zoology* **1982**, *60*, 3377-3386.

31. Borg, B.; Veen, T.V. Seasonal effects of photoperiod and temperature on the ovary of the three-spined stickleback, Gasterosteus aculeatus L. *Can J Zool* **1982**, *60*, 3387–3393, doi:10.1139/z82-428.

32. Bolcun-Filas, E.; Handel, M.A. Meiosis: the chromosomal foundation of reproduction. *Biol Reprod* **2018**, *99*, 112-126, doi:10.1093/biolre/ioy021.

33. Dawe, R.K.; Lowry, E.G.; Gent, J.I.; Stitzer, M.C.; Swentowsky, K.W.; Higgins, D.M.; Ross-Ibarra, J.; Wallace, J.G.; Kanizay, L.B.; Alabady, M.; et al. A Kinesin-14 Motor Activates Neocentromeres to Promote Meiotic Drive in Maize. *Cell* **2018**, *173*, 839-850.e18, doi:10.1016/j.cell.2018.03.009.

34. Dumont, B.L.; Payseur, B.A. Genetic analysis of genome-scale recombination rate evolution in house mice. *PLoS Genetics* **2011**, *7*, e1002116, doi:10.1371/journal.pgen.1002116.

35. Abràmoff, M.D.; Magalhães, P.J.; Ram, S.J. Image Processing with ImageJ. *Biophotonics International* **2004**, *11*, 36–42.

36. Schneider, C.A.; Rasband, W.S.; Eliceiri, K.W. NIH Image to ImageJ: 25 years of image analysis. *Nat Methods* **2012**, *9*, 671–675, doi:10.1038/nmeth.2089.

37. Peichel, C.L.; Ross, J.A.; Matson, C.K.; Dickson, M.; Grimwood, J.; Schmutz, J.; Myers, R.M.; Mori, S.; Schluter, D.; Kingsley, D.M. The master sex-determination locus in threespine sticklebacks is on a nascent Y chromosome. *Curr Biol* **2004**, *14*, 1416–1424, doi:10.1016/j.cub.2004.08.030.

38. Ross, J.A.; Peichel, C.L. Molecular cytogenetic evidence of rearrangements on the Y chromosome of the threespine stickleback fish. *Genetics* **2008**, *179*, 2173–2182, doi:10.1534/genetics.108.088559.

39. Peichel, C.L.; McCann, S.R.; Ross, J.A.; Naftaly, A.F.S.; Urton, J.R.; Cech, J.N.; Grimwood, J.; Schmutz, J.; Myers, R.M.; Kingsley, D.M.; et al. Assembly of the threespine stickleback Y chromosome reveals convergent signatures of sex chromosome evolution. *Genome Biol* **2020**, *21*, 177, doi:10.1186/s13059-020-02097-x.

40. White, M.A.; Kitano, J.; Peichel, C.L. Purifying selection maintains dosage-sensitive genes during degeneration of the threespine stickleback Y chromosome. *Mol Biol Evol* **2015**, *32*, 1981–1995, doi:10.1093/molbev/msv078.

41. Solari, A.J. The spatial relationship of the X and Y chromosomes during meiotic prophase in mouse spermatocytes. *Chromosoma* **1970**, *29*, 217–236, doi:10.1007/bf00326080.

42. Solari, A.J. The behavior of the XY pair in mammals. *Int Rev Cytol* **1974**, *38*, 273–317, doi:10.1016/s0074-7696(08)60928-6.

43. Moses, M.J.; Counce, S.J.; Paulson, D.F. Synaptonemal complex complement of man in spreads of spermatocytes, with details of the sex chromosome pair. *Science* **1975**, *187*, 363–365.

44. Chen, T.R.; Reisman, H.M. A comparative chromosome study of the North American species of sticklebacks (Teleostei: Gasterosteidae). *Cytogenetics* **1970**, *9*, 321-332.

45. Inagaki, A.; Schoenmakers, S.; Baarends, W.M. DNA double strand break repair, chromosome synapsis and transcriptional silencing in meiosis. *Epigenetics* **2010**, *5*, 255-266, doi:10.4161/epi.5.4.11518.

46. Kauppi, L.; Barchi, M.; Baudat, F.; Romanienko, P.J.; Keeney, S.; Jasin, M. Distinct properties of the XY pseudoautosomal region crucial for male meiosis. *Science* **2011**, *331*, 916–920, doi:10.1126/science.1195774.

47. Checchi, P.M.; Engebrecht, J. Heteromorphic sex chromosomes: navigating meiosis without a homologous partner. *Molecular reproduction and development* **2011**, *78*, 623-632, doi:10.1002/mrd.21369.

48. Lisachov, A.P.; Zadesenets, K.S.; Rubtsov, N.B.; Borodin, P.M. Sex chromosome synapsis and recombination in male guppies. *Zebrafish* **2015**, *12*, 174-180, doi:10.1089/zeb.2014.1000.

49. Singer, A.; Perlman, H.; Yan, Y.; Walker, C.; Corley-Smith, G.; Brandhorst, B.; Postlethwait, J. Sex-specific recombination rates in zebrafish (*Danio rerio*). *Genetics* **2002**, *160*, 649–657.

50. Rexroad, C.E.; Palti, Y.; Gahr, S.A.; Vallejo, R.L. A second generation genetic map for rainbow trout (*Oncorhynchus mykiss*). *Bmc Genet* **2008**, *9*, 74, doi:10.1186/1471-2156-9-74.

51. Paigen, K.; Petkov, P. Mammalian recombination hot spots: properties, control and evolution. *Nature Reviews Genetics* **2010**, *11*, 221-233, doi:10.1038/nrg2712.

52. Wong, A.K.; Ruhe, A.L.; Dumont, B.L.; Robertson, K.R.; Guerrero, G.; Shull, S.M.; Ziegle, J.S.; Millon, L.V.; Broman, K.W.; Payseur, B.A.; et al. A comprehensive linkage map of the dog genome. *Genetics* **2010**, *184*, 595-605, doi:10.1534/genetics.109.106831.

53. Broman, K.W.; Murray, J.C.; Sheffield, V.C.; White, R.L.; Weber, J.L. Comprehensive Human Genetic Maps: Individual and Sex-Specific Variation in Recombination. *Am J Hum Genetics* **1998**, *63*, 861–869, doi:10.1086/302011.

54. Paigen, K.; Szatkiewicz, J.P.; Sawyer, K.; Leahy, N.; Parvanov, E.D.; Ng, S.H.S.; Graber, J.H.; Broman, K.W.; Petkov, P.M. The recombinational anatomy of a mouse chromosome. *PLoS Genetics* **2008**, *4*, e1000119, doi:10.1371/journal.pgen.1000119.

55. Jones, D.B.; Jerry, D.R.; Khatkar, M.S.; Raadsma, H.W.; Zenger, K.R. A high-density SNP genetic linkage map for the silver-lipped pearl oyster, *Pinctada maxima*: a valuable resource for gene localisation and marker-assisted selection. *Bmc Genomics* **2013**, *14*, 810, doi:10.1186/1471-2164-14-810.

56. Brelsford, A.; Rodrigues, N.; Perrin, N. High□density linkage maps fail to detect any genetic component to sex determination in a *Rana temporaria* family. *J Evolution Biol* **2016**, *29*, 220–225, doi:10.1111/jeb.12747.

57. Smeds, L.; Mugal, C.F.; Qvarnström, A.; Ellegren, H. High-resolution mapping of crossover and non-crossover recombination events by whole-genome re-sequencing of an avian pedigree. *PLoS Genetics* **2016**, *12*, e1006044, doi:10.1371/journal.pgen.1006044.

58. Acquaviva, L.; Boekhout, M.; Karasu, M.E.; Brick, K.; Pratto, F.; Li, T.; Overbeek, M. van; Kauppi, L.; Camerini-Otero, R.D.; Jasin, M.; et al. Ensuring meiotic DNA break formation in the mouse pseudoautosomal region. *Nature* **2020**, *582*, 426–431, doi:10.1038/s41586-020-2327-4.

59. Soriano, P.; Keitges, E.A.; Schorderet, D.F.; Harbers, K.; Gartler, S.M.; Jaenisch, R. High rate of recombination and double crossovers in the mouse pseudoautosomal region during male meiosis. *Proc National Acad Sci* **1987**, *84*, 7218-7220, doi:10.1073/pnas.84.20.7218.